Deep Learning Based Radio Frequency Fingerprint Identification by Exploiting Spatial Stereoscopic Features

Shunliang Zhang[1,2], Jing Li[1,2], and Xiaolei Guo[1,2(✉)]

[1] Institute of Information Engineering, Chinese Academy of Sciences, Beijing, China
{zhangshunliang,lijing,guoxiaolei}@iie.ac.cn
[2] School of Cyber Security, University of Chinese Academy of Sciences, Beijing, China

Abstract. The unique radio frequency fingerprint (RFF) resulting from hardware imperfections can be used to identify wireless devices to resist impersonating or spoofing attacks. The existing methods for RFF identification typically rely on the transient or steady-state features of RF signals. However, the limited number of extracted features affects the performance of radio device identification, which is not satisfactory. This paper proposes a spatial stereoscopic feature extraction method that transforms the three statistical features based on radio signal frequency envelopes into three-dimensional images to address this issue. By increasing the dimensionality, it can improve the quantity of features. Additionally, we propose a multi-channel parallel convolutional neural network (MPCNN) for classifying devices based on the spatial stereoscopic features. Experimental results demonstrate that our proposed method outperforms benchmark approaches in terms of identification accuracy. Specifically, it achieves mobile device identification with an accuracy higher than 99% even with a small sample size.

Keywords: Deep learning · Device identification · RFF · MPCNN

1 Introduction

The widespread deployment of Internet of Things (IoT) devices greatly enhances people's daily lives. However, the broadcast nature of wireless communications introduces security and privacy concerns. Most existing wireless communication systems achieve security through upper-layer mechanisms, which may not be suitable for emerging wireless communication scenarios like IoT due to the computational and power limitations of the devices [1]. As a Physical layer security (PLS) technique, physical layer authentication (PLA) enables a receiver to verify the identity of a transmitter using physical layer attributes of received signals, such as channel and radio frequency (RF) characteristics. The unique fingerprint derived from the features of electromagnetic waves emitted by the transmitter can be used to identify wireless devices. Due to inherent hardware imperfections

A. Zaslavsky et al. (Eds.): MobiQuitous 2023, LNICST 594, pp. 511–519, 2024.
https://doi.org/10.1007/978-3-031-63992-0_34

caused by manufacturing and environmental factors, device-dependent deviations from ideal hardware can result in unique features of transmitted electromagnetic waves. Tampering with the RF fingerprint (RFF) is very difficult, making it suitable for device identification to defend against attacks.

The RFF-based PLA is applicable for device classification and identification in the IoT environment since it doesn't rely on complex cryptography operations or third-party authentication. Machine learning (ML) methods have been extensively used for RFF identification (RFFI), but their performance depends on manual feature engineering and is limited in different radio environments. Traditional ML methods also struggle with a large number of targets [2], making them unsuitable for the 6G system with massive IoT/IoV devices. Deep learning (DL) methods can extract more distinguishing RF fingerprints and show promise in improving RFF-based identification [3]. Combining transient-state and steady-state signal features in RFFI is a potential approach since both types have their strengths and weaknesses. However, conventional statistical learning or ML methods struggle to automatically select influential features by removing irrelevant or redundant features from different RF signals.

Motivated by this situation, this paper proposes a DL-based method to identify mobile devices based on spatial stereoscopic images constructed using statistical features of three-dimensional (3D) RF signals from both the transient state and steady state. The construction of spatial stereoscopic feature images improves the quantity of sample features and reduces the reliance on sample size. The main contributions of this paper are as follows:

- We developed a novel method for the extraction and representation of RF fingerprint features. Specifically, 3D features are extracted from RF signals in both the transient state and the steady state, and these features are constructed as spatial stereoscopic images.
- A multi-channel parallel CNN algorithm is developed to train models and classify RF fingerprints based on their spatial characteristics.
- We verified the performance of the proposed method through extensive simulations, and compared it with benchmark methods to highlight its advantages in terms of identification accuracy and sample size.

2 Related Work

IoT devices with limited computing and power make it difficult for traditional ML algorithms and upper-layer mechanisms to meet the security and reliability requirements of future B5G/6G systems. DL-based RFF recognition ensures the security of upcoming 6G systems [4]. Comparative analysis shows that DL-based methods outperform traditional ML methods in identification accuracy [5].

2.1 RFFI Based on Constellation Maps

A constellation map is an image representation of the statistical characteristics of modulation signals, which has been utilized by many studies as RFF fingerprint features for RFF identification. Peng et al. [6] employed the differential

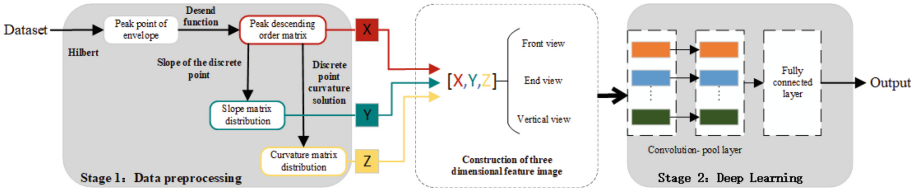

Fig. 1. Experimental framework

constellation map as the recognition feature for CNN, successfully classifying 99 Zigbee devices and evaluating RF fingerprint recognition performance under different signal-to-noise ratio (SNR) conditions. Yang et al. [7] utilized the differential constellation trajectory diagram algorithm to extract RF fingerprints. While the RFFI method based on constellation maps achieves high recognition accuracy to some extent, it is highly dependent on the SNR. When the SNR falls below a certain threshold, statistical features based on constellations degrade, consequently impacting the recognition performance.

2.2 RFFI Based on Spectral Graph

Spectral maps exhibit fine-grained time-frequency characteristics and have shown good classification performance in the RFFI scheme based on spectral graphs. Shen [8] successfully classified and recognized 20 LoRa devices using spectrum diagrams and CNNs. The experiment revealed that the RF fingerprint based on spectrum diagrams has a certain level of uniqueness and outperforms schemes based on I/Q data and FFT [9]. By converting the one-dimensional time-domain format of wireless signals into 2D spectral images, the characteristics of the spectral map are derived as RF fingerprints. VGG-16 is employed to identify RF fingerprints, resulting in the recognition of 20 different wireless transmitters [10]. With the advancement of DL, researchers have proposed new RF fingerprint feature extraction methods tailored to specific scenarios. For instance, [11] developed an SCCNN-based RFFI for civil aircraft ADS-B equipment.

3 RFF Identification Framework

3.1 The Proposed Framework

Figure 1 outlines the proposed DL-based framework for RFFI. The framework consists of two stages: RF signal preprocessing and RFFI. The 3D feature images generated from the first state are used as input for device identification in the second stage.

Phase 1: Data preprocessing and 3D image construction. The spatial stereoscopic features are constructed based on the complete envelope of radio frequency signals, including transient and steady-state features. Firstly, the envelope distribution points of the RF signal are extracted. Subsequently, the descending

arrangement of envelope distribution, slope feature distribution, and curvature feature distribution are obtained. Finally, the spatial image is constructed by using the obtained 3D features.

Phase 2: Space stereoscopic feature-based device identification. The 3D feature images obtained in stage 1 are used as input into the multi-channel parallel convolutional neural network model (MPCNN) for device identification and classification. Specifically, the three views of the 3D images are used as input to the three channels respectively for device identification.

3.2 Data Preprocessing

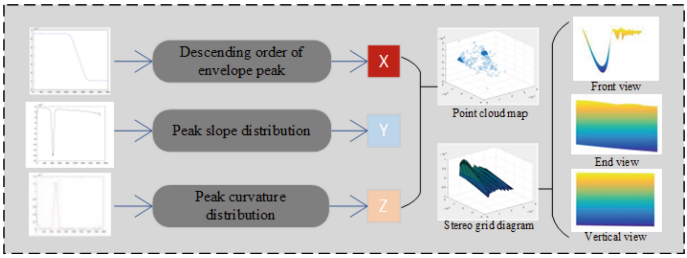

Fig. 2. Spatial stereo feature image construction

The data used in this experiment is from public datasets [12]. As shown in Fig. 2, data preprocessing consists of four steps as follows.

Step 1: The peak point of signal envelope extraction. The typical methods to extract the peak point of the signal envelope include the Hilbert, square energy, and Shannon energy. In this experiment, Hilbert's principle is used, and the specific solution is based on Formula 1. The input signal is denoted by $x(t)$. The Formulas 2 and 3 represent the peak points and the descending arrangement respectively.

$$\hat{x(t)} = H[x(t)] = X(t) * \frac{1}{\pi t} \tag{1}$$

$$P_n = peaks\left\{x(t) + j\hat{x(t)}\right\}, (n = 1....N) \tag{2}$$

$$D_n = Descend\{P_n\} = [x_n, y_n] \tag{3}$$

Step 2: Slope feature extraction. Since the envelope obtained in Step 1 is distributed as discrete points, the slope feature of the envelope distribution can be derived using the slope of these points, as shown in Formula 4.

$$\frac{y_n - y_{n-1}}{x_n - x_{n-1}} = k_i, (i = 1, 2...n) \tag{4}$$

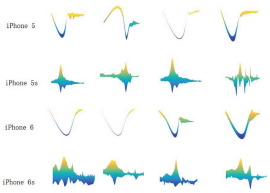

Fig. 3. Front view of 3D feature images

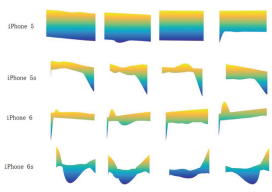

Fig. 4. End view of 3D feature images

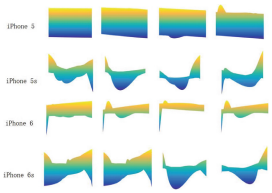

Fig. 5. Vertical view of 3D feature images

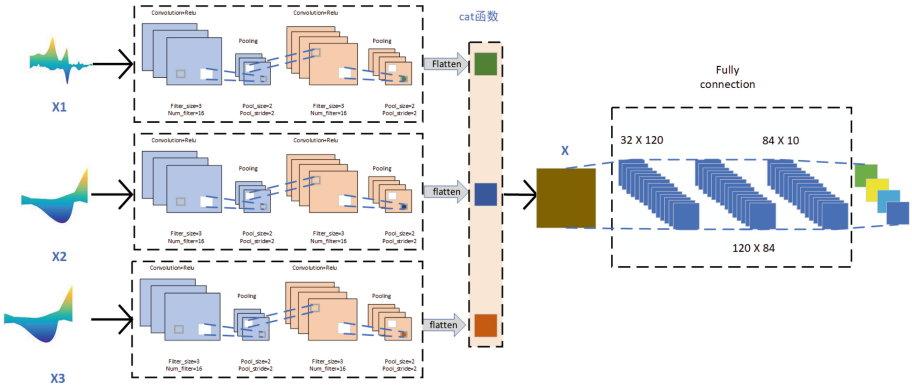

Fig. 6. Multi-channel parallel CNN model

Step 3: Curvature feature extraction. Similar to the slope feature extraction, the curvature feature extraction is also based on discrete point curvature. Two algorithms are proposed to derive the curvature features from discrete points.

Theorem 1. *The curvature of the curve derived from three non-collinear points can be determined by approximating it to a circle using the tangent line of the three-point vector distance. The Formula 5 demonstrates the calculation of curvature. Assuming the vector distances between these points are denoted as a and b. Based on the vector distance, Formula 6 can be used to calculate the curvature of discrete points and obtain the curvature distribution.*

$$k = \frac{\left| x'' y' - x' y'' \right|}{(x')^2 + (y')^2} \tag{5}$$

$$k = \frac{2(a_3 b_2 - a_2 b_3)}{(a_2^2 + b_2^2)^{\frac{3}{2}}} \tag{6}$$

Theorem 2. *The curvature circle can be constructed using the three non-collinear points, and the radius of the circle can be obtained. According to the relationship between the radius and the curvature, the curvature can be derived as* $k = 1/R$.

Step 4: 3D image construction and three views extraction. The three envelope peak feature points from previous steps are inputted as X, Y, and Z coordinates. The scatter function processes the 3D scatter images, which are then used for grid-based 3D image construction. Three views of the 3D image are extracted using the view function, as depicted in Figs. 3, 4, and 5.

3.3 Multi-channel Parallel CNN Model

The RF signal features are represented as spatial stereoscopic images, and three views (front, side, and top) are used to extract spatial features. These three views serve as inputs to the multi-channel parallel CNN model. In Fig. 6, X_1, X_2, and X_3 undergo two convolution and pooling layers in each channel. The flatten function normalizes the obtained feature vectors, and the cat function concatenates the normalized feature vectors. The comprehensive feature, denoted as X, is obtained from these three-channel feature vectors. Three fully connected layers are used to connect the comprehensive feature X. Finally, the model outputs the features of the three input images from the three channels.

4 Experiment Evaluation

4.1 Evaluation Metrics

The identification accuracy in the test stage is defined as Formula 7.

$$\text{Accuracy} = \frac{TP + TN}{TP + TN + FP + FN} \tag{7}$$

There are four categories of classification, "TP" stands for true positive of positive class, "TN" stands for true positive of negative class, "FP" stands for false positive of positive class, and "FN" stands for false positive of negative class.

4.2 Experiment Design

Exp. I: The identification accuracy of mobile phones. Mobile devices from two famous manufacturers including Samsung and Apple are used in the experiment. Specifically, 7 different models of iPhone devices and 4 different models of Samsung devices are selected for identification. The stereo feature images extracted from these devices are classified and identified. The effectiveness of the proposed method is evaluated according to the identification accuracy.

Exp. II: The impact of sample size. By comparing several previous RFFI methods based on the CNN model for image construction with different RF characteristics, the experiment evaluates the performance of the proposed method compared with existing benchmark solutions.

4.3 The Performance of MPCNN on Device Identification

Algorithm 1 is used to calculate the curvature of discrete points with three-point parameters, and algorithm 2 is used to solve the curvature of discrete points with the three-point fixed circle.

Table 1. Device identification accuracy based on algorithm 1

Device of type	Training acc.	Test accuracy	Average acc.
iPhone5	99.84%	99.73%	99.63%
iPhone5s	97.32%	98.77%	97.61%
iPhone6	99.36%	99.39%	99.37%
iPhone6s	100%	99.80%	99.96%
iPhone7	99.77%	99.64%	99.74%
iPhone7plus	99.85%	99.62%	99.80%
Note3	99.22%	99.00%	99.18%
S3	99.57%	99.87%	99.63%
S4	99.15%	99.71%	99.26%
Average Acc.	99.44%	99.46%	99.42%

Table 2. Device identification accuracy based on Algorithm 2

Device of type	Training acc.	Test accuracy	Average acc.
iPhone5	97.99%	96.31%	97.65%
iPhone5s	96.21%	95.54%	96.08%
iPhone6	96.39%	95.46%	96.20%
iPhone6s	98.24%	97.58%	98.11%
iPhone7	96.17%	96.15%	96.11%
iPhone7plus	95.53%	94.11%	95.25%
Note3	99.57%	98.84%	99.42%
S3	100%	99.80%	99.96%
S4	96.97%	91.14%	95.80%
Average Acc.	97.47%	96.43%	97.21%

Tables 1 and 2 display the device classification accuracy of the proposed MPCNN method. The input for this method includes spatial stereoscopic feature images obtained from algorithm 1 and algorithm 2 respectively. The performance of the proposed method utilizing these two curvature calculation methods achieves an accuracy of over 95%. Additionally, the MPCNN's classification accuracy using input from algorithm 1 reaches 99%, surpassing the accuracy of input from algorithm 2. This is because algorithm 2 forcibly determines curvature circles, resulting in a loss of curvature features and a decrease in the representativeness of the constructed spatial features.

Table 3. Identification performance of different CNN+RFF methods

Num.	Target	Feature	Dataset	ACC.
1	Smartphone (Blutooth)	Spatial stereoscopic feature image	1650	99.42%
2	Smartphone	PRACH preamble	878	96.33%
3	LoRa	Spectral diagram	1000	97.61%
4	Zigbee	constellation diagram	24300	99.1%
5	USRP	I/Q	399360	99.86%
6	WiFi	I/Q waveform	402000	95%

4.4 The Influence of Sample Size

Table 3 shows the performance of existing CNN-based RFFI methods using various RF signal features. CNN-based RFFI methods utilizing spatial stereoscopic feature images achieve the second-best performance, showcasing the advantages of the proposed RF signal feature extraction and representation method. Figure 7 compares the performance of existing CNN-based RFFI methods and the proposed method with different sample sizes. RFFI methods based on differential constellation maps and I/Q sequences require a sample size of 10^6 for target performance. In contrast, the RFFI method based on the spectrum diagram and PRACH leading code requires a similar sample size as the proposed method for achieving the claimed performance. The latter three methods require considerably smaller sample sizes compared to the former three methods. Furthermore, as depicted in Fig. 8, the proposed method outperforms the other two existing methods (spectrum diagram and PRACH leading) in identification accuracy with a similar sample size. Through comprehensive analysis, it is evident that the proposed method can achieve nearly ideal identification accuracy with a very small sample size, making it more suitable for scenarios with limited practical radio environment samples.

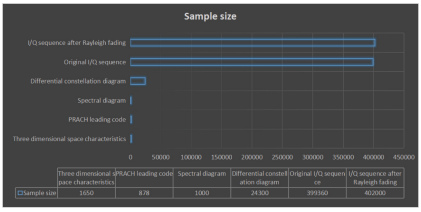

Fig. 7. Sample size comparison

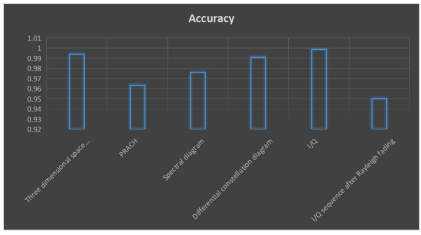

Fig. 8. Accuracy comparison

5 Conclusion

This paper proposes a novel MPCNN-based RFFI method and a new method to construct spatial 3D features from the radio-frequency signal envelope. This method enhances the feature dimension and quantity by constructing multiple features in a three-dimensional space. Simulation results indicate that this approach solves the practical issue of improving recognition performance with limited data samples, while also reducing the complexity of RF signal data preprocessing.

Acknowledgment. This work is funded by the National Key Research and Development Program of China under Grant No. 2021YFB2910103.

References

1. Xie, N., Li, Z., Tan, H.: A survey of physical-layer authentication in wireless communications. IEEE Commun. Surv. Tutorials **23**(1), 282–310 (2021)
2. Peng, L., Zhang, J., Liu, M., Hu, A.: DL based RFFI using differential constellation trace figure. IEEE Trans. Veh. Technol. **69**(1), 1091–1095 (2020)
3. Yu, J., Hu, A., Li, G., Peng, L.: A robust RF fingerprinting approach using multisampling convolutional neural network. IEEE Internet Things J. **6**(4), 6786–6799 (2019)
4. Pan, Y., Yang, S., Peng, H., et al.: Specific emitter identification based on deep residual networks. IEEE Access **7**, 54425–54434 (2019)
5. Youssef, K., Bouchard, L., Haigh, K., et al.: Machine learning approach to RF transmitter identification. IEEE J. Radio Freq. Identif. **2**(4), 197–205 (2018)
6. Peng, L., Zhang, J., Liu, M., Hu, A.: Deep learning based RFFI using differential constellation trace figure. IEEE Trans. Veh. Technol. **69**(1), 1091–1095 (2020)
7. Yang, T., Zhao, J., Wang, X., Xu, F.: Deep learning based RFF recognition with differential constellation trace figure towards closed and open set. IEEE/CIC International Conference on Communications in China (ICCC), pp. 908–913 (2022)
8. Shen, G., Zhang, J., Marshall, A., Peng, L., Wang, X.: Radio frequency fingerprint identification for LoRa using spectrogram and CNN. In: IEEE Conference on Computer Communications (INFOCOM), pp. 1–10 (2021)
9. Shen, G., Zhang, J., Marshall, A., et al.: Radio frequency fingerprint identification for LoRa using deep learning. IEEE J. Sel. Areas Commun. **39**(8), 2604–2616 (2021)
10. Zong, L., Xu, C., Yuan, H.: A RF fingerprint recognition method based on deeply convolutional neural network. In: IEEE Information Technology and Mechatronics Engineering Conference (ITOEC), pp. 1778–1781 (2020)
11. Li, J., Ying, Y., Wang, S., et al.: Slice combination convolutional neural network based radio frequency fingerprint identification for Internet of Things. Wireless Netw. **29**, 1–14 (2023). https://doi.org/10.1007/s11276-023-03241-8
12. Hall, E.S., Vawdrey, D.K., Knutson, C.D., et al.: Enabling remote access to personal electronic medical records. IEEE Eng. Med. Biol. Mag. **22**(3), 133–139 (2003)